Thrombospondin-1 mimetics are promising novel therapeutics for MYC-associated medulloblastoma

Tiffany S. Y. Chan, **Daniel Picard, Cynthia E. Hawkins, Mei Lu, Stefan Pfister, Andrey Korshunov, Martine F. Roussel, Robert J. Wechsler-Reya, Jack Henkin, Eric Bouffet, and Annie Huang**

Department of Pediatrics, Laboratory Medicine and Pathobiology, University of Toronto, Toronto, Ontario, Canada (T.S.Y.C., D.P., E.B., A.H.); Arthur and Sonia Labatt Brain Tumour Research Center, The Hospital for Sick Children, Toronto, Ontario, Canada (T.S.Y.C., C.E.H., M.L., A.H.); Department of Pathology, The Hospital for Sick Children, Toronto, Ontario, Canada (C.E.H.); Division of Pediatric Neurooncology, Clinical Cooperation Unit Neuropathology, German Cancer Research Center (DKFZ), Department of Pediatric Oncology, Hematology and Immunology, University Hospital Heidelberg, Heidelberg, Germany (S.P., A.K.); Department of Tumour Cell Biology, St. Jude Children's Research Hospital, Memphis, Tennessee, USA (M.F.R.); Sanford-Burnham Medical Research Institute, La Jolla, California, USA (R.J.W.); Department of Chemistry, Northwestern University, Evanston, Illinois, USA (J.H.)

Corresponding Author: Annie Huang, MD, PhD, Department of Pediatrics, Laboratory Medicine and Pathobiology, Arthur and Sonia Labatt Brain Tumour Research Center; The Hospital for Sick Children, 555 University Avenue, Toronto, ON M5G 1X8, Canada (annie.huang@sickkids.ca).

Abstract

Background. Medulloblastoma (MB) comprises four subtypes of which group 3 MB are the most aggressive. Although overall survival for MB has improved, the outcome of group 3 MB remains dismal. C-*MYC (MYC)* amplification or MYC overexpression which characterizes group 3 MB is a strong negative prognostic factor and is frequently associated with metastases and relapses. We previously reported that MYC expression alone promotes highly aggressive MB phenotypes, in part via repression of thrombospondin-1 (TSP-1), a potent tumor suppressor.
Methods. In this study, we examined the potential role of TSP-1 and TSP-1 peptidomimetic ABT-898 in *MYC*-amplified human MB cell lines and two distinct murine models of MYC-driven group 3 MBs.
Results. We found that TSP-1 reconstitution diminished metastases and prolonged survival in orthotopic xenografts and promoted chemo- and radio-sensitivity via AKT signaling. Furthermore, we demonstrate that ABT-898 can recapitulate the effects of TSP-1 expression in MB cells in vitro and specifically induced apoptosis in murine group 3 MB tumor cells.
Conclusion. Our data underscore the importance of TSP-1 as a critical tumor suppressor in MB and highlight TSP-1 peptidomimetics as promising novel therapeutics for the most lethal subtype of MB.

Key Point

- Therapeutic role of TSP-1 in Medulloblastoma; TSP-1 mimetics targets MYC-PI3K/AKT oncogenic axis.

Medulloblastoma (MB) is the most common pediatric malignant brain tumor.[1] Advance in therapy have improved overall survival to nearly 80% for patients with localized disease, however, survivors often suffer from significant disease and treatment-induced short and long-term toxicity.[2] Importantly, metastatic and recurrent MBs are still highly fatal diseases, for which no effective therapies are currently available.

Cumulative genomic studies have identified four molecular subtypes of MB,[3] of which the WNT subtype has the most favorable prognosis while group 3/4 MB has the poorest

Importance of the Study

Our study shows that silencing of TSP-1 contributes significantly to the metastatic, chemo- and radiation-resistant phenotypes seen in Myc driven MB. More importantly, TSP-1 peptidomimetic ABT-898 suppresses pro-survival PI3K/AKT signaling activities, and promotes apoptosis in 2 Myc-driven murine MB models suggesting it to be a promising novel pharmacological treatment for these aggressive MB tumors.

prognosis. Patients with group 3/4 MB often develop resistance to standard therapy and have higher chances of relapse.[4,5] *MYC* amplification or hyper-activation is a hallmark of group 3 MB and is a strong prognostic factor for poor survival.[4] Recently, 2 murine models of MYC-driven group 3 MB have been established using mouse neural stem cells or neuronal precursor cells, and serve as excellent therapeutic models.[6,7] Murine studies indicate PI3K/AKT signaling is a critical driver in MYC-driven MB,[7] and also contributes to metastasis in Sonic Hedgehog-induced MB.[8] However, mechanisms by which MYC and Phosphoinositide 3-kinase (PI3K)/protein kinase B (AKT) pathway promote metastatic phenotypes in MB remain incompletely elucidated.

Thrombospondin *(TSP)-1*, which encodes a matrix-cellular glycoprotein, is a powerful tumor suppressor that is negatively regulated by several oncogenic pathways including Ras[9] and MYC[10,11], via PI3K signaling[12] and is frequently down-regulated in malignant and metastatic tumors. Expression of TSP-1 protein has potent tumor-suppressive activity and inhibits malignant growth and metastasis in a variety of cancer models.[9,13,14] In addition to its well-recognized anti-angiogenic function, TSP-1 affects tumor suppression via various mechanisms including cell adhesion, differentiation, migration, and apoptosis.[15–17] TSP-1 is a complex modulator with multiple functional domains that interact with different receptor proteins, including CD36 and β1-integrins to affect signaling. The TSR epitope repeat 1, which is the best characterized of TSP-1 domains is linked to multiple cellular effects including cell adhesion, apoptosis and angiogenesis, and has been intensively investigated as a candidate pharmacologic mimetic. Several generations of pharmacologically active TSP-1 peptidomimetics (ABT-510, ABT-526, and ABT-898) which mimic the TSR repeat 1 have been developed and shown to have promising anti-angiogenic, pro-apoptotic[13,14] and chemo-sensitizing effects[15,16] in vivo and cell lines.

We previously reported MYC promotes highly aggressive and metastatic MB phenotypes, in part via regulation of cell differentiation and migratory transcriptional programs.[18] Our studies identified TSP-1 as a robust direct transcriptional target of MYC and showed that reconstitution of TSP-1 attenuated MYC-induced cell migration and transformation in vitro.[18] In this study, we sought to further elucidate the tumor-suppressive role of TSP-1 in MB and investigated the potential therapeutic role for TSP-1 using in vivo orthotopic xenograft models, and engineered MYC-driven MB. Significantly our study shows that TSP-1 is a potent suppressor of metastases and prolongs survival in orthotopic MYC-driven MB models. Using *MYC*-amplified human tumor cell lines and two independent murine

models of MYC-driven group 3 MB, we also show that TSP-1 promotes chemo- and radio-sensitivity via AKT signaling in MB cells. Significantly, these effects were re-capitulated by TSP-1 peptidomimetic, ABT-898, which also induced apoptosis in the 2 distinct murine group 3 MB tumor cells. Collectively, our data underscore the functional importance of TSP-1 in MB and highlight peptidomimetics of TSP-1 as a promising novel therapeutics for high-risk MB.

Material and Methods

Cell Culture

Human group 3 medulloblastoma established cell lines D283, D458, D458-TSP-1 (American Type Culture Collection) were maintained in zinc option medium (Life Technologies); and UW426-MYC were maintained in αMEM containing 10% fetal bovine serum (FBS). MP mouse tumor cells (human *MYC-T58A & Trp53DN*- infected neural stem cells; from Dr. Wechsler-Reya, Sanford-Burnham Medical Research Institute) were maintained in Neurocult complete medium with FGF1, EGF, and N2 supplements (Stem Cell Technologies) as described previously.[7] G3 mouse MB cells (human *MYC*-infected *Trp53-/-; Cdkn2c-/-* GNPs) and Sonic Hedgehog (SHH) mouse MB (*Ptch1+/- Trp53-/-* GNPs) from Dr. Roussel, St. Jude Children's Research Hospital, TN, were maintained as neurospheres in neurobasal medium with FGF1, EGF, B27 and N2 supplements as previously reported.[6]

Cell Proliferation, Death and Migration Assays

Cell proliferation was assessed using MTS assays (Roche Colorimetric Cell Proliferation) at regular intervals as described previously,[18] and results were verified by direct Trypan blue cell count.

Cell death was assessed using MTS assays, Western blot analyses for cleaved poly-(ADP-ribose) polymerase (PARP), and in situ TdT-mediated dUTP-biotin nick end labeling (TUNEL) assays. In brief, cells were first seeded under normal growth conditions (10% FBS), and then (i) starved 24 h later by replacing the medium with low serum (0.1% FBS) medium, (ii) treated with different chemotherapeutic reagents, (iii) or exposed to gamma-irradiation. Western-blotting was performed to measure the level of cleaved PARP as a biochemical indication of caspase-mediated apoptosis.

TUNEL assay was performed as described using in situ cell death detection kit (Roche Applied Science) in accordance with the manufacturer's protocol. In brief, cells seeded on slides were stressed for 48 and 72 h and were

fixed with 4% paraformaldehyde in 0.1M phosphate buffer, followed by incubation with TUNEL reaction mixture for 60 min at 37°C. Reactions were stopped, and biotin-dUTP was incorporated for detection.

Matrigel invasion assay was performed as previously described[18] using a Transwell Boyden chamber assay according to the manufacturer's instructions (BD Sciences, Franklin Lakes). In brief, 3.5×10^4 cells were seeded in chambers and grown at 37°C for 18–40 h. To quantify migrated cells, membranes were stained with 1% toluidine, migrated cell counts were determined based on 10 random microscopic fields.

Tumor Materials

Medulloblastoma tissue microarrays used in this study were constructed at the Hospital for Sick Children, and German Cancer Research Center. Immuno-reactivity for TSP-1 (Antibody used: TSP-1 monoclonal antibody (1:1000; Abcam)) was scored manually based on intensity (1 = low, 2 = mod, 3 = high) and distribution of stains (1 = ≤10%, 2 = 10–50%, 3 > 50%). Immunohistochemical (IHC) values were determined based on the average staining score of at least 2 tissue cores. All IHC stains were scored blindly by T.C. and D.P., and reviewed by C.H.

Orthotopic Xenograft Assays

NOD-SCID mice were maintained in accordance with the Hospital for Sick Children institutional animal care committee approved protocols. Briefly, cerebella of 4–6-week-old anesthetized male mice (Charles River, Quebec, Canada) were injected stereotactically with 1×10^5 stable TSP-1 expressing UW426-MYC/D458 cells. All animals were euthanized as per standard tumor endpoint monitoring guidelines. Histopathologic analyses of the whole brain and spine from all mice were performed.

Histology and Immunohistochemistry

Immunohistochemistry was performed on formalin-fixed paraffin-embedded tissues using standard procedures. Xenograft tissues were subjected to antigen retrieval by pressure cooking (citrate buffer, pH 6, 20 min) and 0.3% H_2O_2 endogenous peroxidase blocking. For primary antibody: TSP-1 monoclonal antibody (1:1000; Abcam), CD31 monoclonal antibody (1:500; Millipore), Ki-67 (1:150; Dako, Agilent Technologies), were incubated overnight at 4°C, treated with bio-tinylated secondary IgG antibodies for 30 min using ABC reagent kit and DAB chromagen (Vector Laboratories). A final counterstain was performed in hematoxylin followed by serial dehydration in ethanol and xylene and mounted in Permount (Thermo Fisher Scientific). Hematoxylin and eosin (H&E) stains were performed using standard protocols.

Immunoblot Analyses

Cell proteins lysates were performed using standard EBC whole cell lysis buffer as described previously,[19] and analyzed by Western blotting with TSP-1 (1:500, Abcam), MYC (1:500, in-house 9E10 monoclonal), α-tubulin (1:5,000; Sigma-Aldrich), α-PARP, α-p-AKT308, α-pan-AKT, α-pThr202/Tyr204ERK1/2, α-ERK1/2 (1:1,000; Cell SignallingTechnology), and antispecies horseradish peroxidase-conjugated antibodies (Bio-Rad Laboratories). Detection was performed using Chemiluminescence Reagent Plus (PerkinElmer).

Informatic and Statistical Analysis

The log-rank analysis was performed using the Kaplan–Meier method to determine significance of survival differences in the tumor xenograft studies. Significance for in vitro cell growth/death/migration data was determined using the Student's two-tailed *T*-test (N.S. = not significant; $*P$-value < .05; $**P$-value < .01).

Results

Thrombospondin-1 Expression Correlates with Favorable Medulloblastoma Biology

In order to investigate the clinical relevance of TSP-1 in human MB, we performed IHC analysis in 326 primary human MBs and examined TSP-1 expression relative to patient age, gender, metastatic, and recurrence status (Table 1). High TSP-1 expression was observed in 21.2% (69/326) of primary MBs. Notably, the extent of TSP-1 expression correlated with MB molecular subgroups. A significantly greater proportion of the favorable WNT MB exhibited high TSP-1 expression as compared to other MB subtypes. High TSP-1 expression was observed in 50% (9/18) of WNT tumors as compared to 23.2% (22/95) of SHH, 17.4% (12/69) of group 3 and 19.2% (20/104) of group 4 tumors (P = .006). TSP-1 expression also correlated significantly with metastatic status; 25.9% (54/208) of nonmetastatic MBs exhibited TSP-1 immuno-positivity while a majority of metastatic tumors (86.1%; 93/108) exhibited minimal TSP-1 expression (P = .019).

Thrombospondin-1 Inhibits Medulloblastoma Tumor Progression and Metastases In Vivo

Since re-expression of TSP-1 inhibited MB transformation and cell migratory phenotypes in vitro,[18] we postulated that TSP-1 may attenuate metastatic MB phenotypes in vivo. To investigate the TSP-1 tumor-suppressive role in vivo, we characterized the effects of stable TSP-1 expression in UW426-MYC and in D458, an MB cell line with *MYC* amplification using orthotopic xenograft assays. We observed that mice harboring TSP-1 expressing xenografts had significantly longer survival than control animals. Mice bearing UW426-MYC-TSP-1 and D458-TSP-1 xenografts survived 28.8 ± 5.3 and 68 ± 8.2 days respectively while survival time of mice bearing UW426-MYC-vector and D458-vector control xenografts was 21.9 ± 2.5 and 38.5 ± 10.3 days, respectively (Figure 1A). Notably, D458-TSP-1 and UW426-MYC-TSP-1 xenografts were significantly smaller than control xenografts (P < .05, Figure 1B, C, Supplementary Figure 1), and associated with the diminished incidence of

Table 1. Correlation of TSP-1 Expression With Clinicopathological Features in MB

	TSP1 **Negative**	TSP1 **Positive**	*P*-value
n = 326	257 (78.8%)	69 (21.2%)	
Age (years old)			
<3	53 (81.5%)	12 (18.5%)	.614
>3	203 (78.1%)	57 (21.9%)	
Sex			
Female	158 (76.7%)	48 (23.3%)	.196
Male	98 (82.3%)	21 (17.6%)	
Metastasis			
M0	154 (74.0%)	54 (25.9%)	.019
M+	93 (86.1%)	15 (13.9%)	
Recurrence			
No	176 (76.2%)	55 (23.8%)	.131
Yes	77 (94.6%)	14 (15.4%)	
Status			
Alive	193 (77.2%)	57 (22.8%)	.204
Dead	64 (84.2%)	12 (15.8%)	
Molecular subgroup			
WNT	9 (50.0%)	9 (50.0%)	.006
SHH	73 (76.8%)	22 (23.2%)	(WNT vs non-WNT)
3	57 (82.6%)	12 (17.4%)	
4	84 (80.8%)	20 (19.2%)	

metastases. Only 20–28.5% of TSP-1 expressing xenografts exhibited spinal metastases as compared to 63–66.6% of the control groups (*P* < .05, Figure 1B, D).

To further understand the mechanism underlying TSP-1 associated antitumor effects in MB xenografts, we performed human-specific Ki-67 IHC analyses and interestingly observed no significant difference in proliferative indices between control and TSP-1-expressing tumors (Figure 2A, B). Given the known role of TSP-1 in regulating angiogenesis and the tight relationship between tumor metastasis and angiogenesis,[10] we assessed whether the antimetastatic effect of TSP-1 correlated with neo-vascularization as measured by microvessel density (MVD) analysis in both MB xenografts and primary human MBs. Using CD31 as a surrogate to evaluate neo-vascularization, we observed that TSP-1 expression did not correlate with MVD in MB xenografts (*n* = 40, *P* = .68, Figure 2A, C). MVD in TSP-1 positive and negative human MB tumors (*n* = 260) were also not significantly different (Figure 2D, E). These findings suggest that the antimetastatic properties of TSP-1 in MB are independent of its antiangiogenic properties.

Thrombospondin-1 Peptidomimetic ABT-898 Targets PI3K/AKT Signaling to Inhibit Medulloblastoma Cell Migration and Invasion

To define the mechanism of TSP-1 antimetastatic effect in MB, we investigated the effect of TSP-1 expression on 2 major oncogenic signaling pathways (PI3K and MAPK) implicated in MYC-dependent MB metastases[7,20] as well as the Rac/Rho GTPase pathways which regulates cell migration.[21] Immunoblotting

analyses showed phospho-AKT-T308 expression was significantly diminished with TSP-1 overexpression without any changes in total or phosphorylated ERK1/2, Rac1,2,3, or CDC42 expression, thus indicating TSP-1 specifically altered PI3K/AKT signaling in group 3 MB cell lines (Figure 3A).

To investigate the potential therapeutic effects of TSP-1, we next examined whether ABT-898, a pharmacologic peptidomimetic of the TSR domain could recapitulate the biological effects of TSP-1 protein expression on MB cell phenotypes and PI3K/AKT signaling. We observed that ABT-898 did not alter the viability of UW426-MYC, D458, or D341 cells (Figure 3B; Supplementary Figure 2), but specifically diminished migration/invasion activity in UW426-MYC, D458, and D341 cells by up to 80% in a dose-dependent manner as compared to controls (Figure 3C). Importantly, ABT-898 treatment also diminished phospho-AKT expression in UW426-MYC and D458 cells in a dose-dependent manner (Figure 3D) without affecting phosphor- or total ERK1/2 expression, once again indicating the specific inhibitory effects of ABT-898 on PI3K/AKT signaling and on MB cell migration. Of note, although TSP-1 has been reported to modulate MYC expression via CD47 signaling,[13,22] in our study MYC expression remained unchanged upon TSP-1 reconstitution or ABT-898 treatment (Figure 3A, D) and indicate MYC maps upstream of TSP-1 in MB.

ABT898 Enhances Chemo-and Radio-Sensitivity in Medulloblastoma Cells

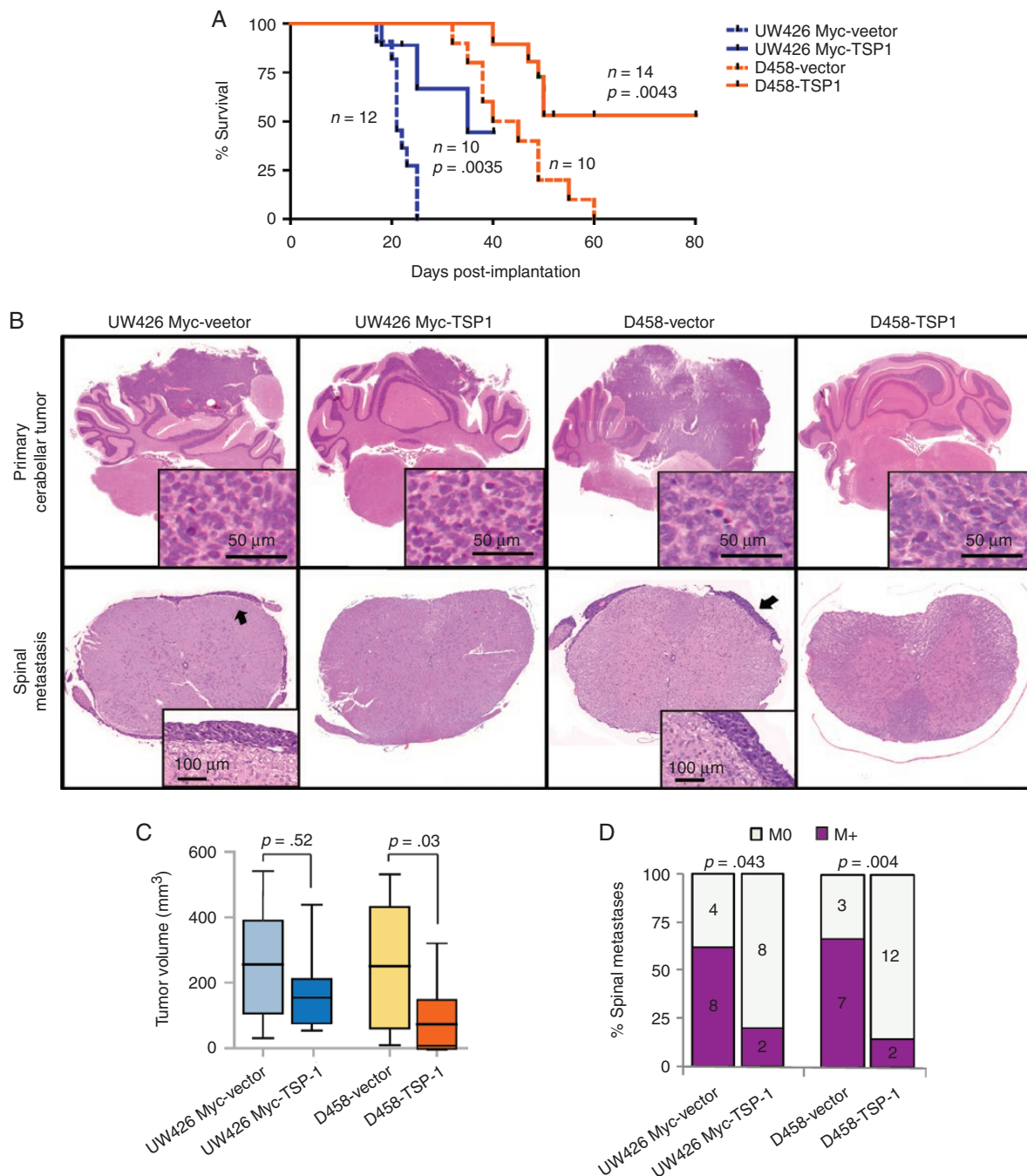As TSP-1 is known to activate apoptotic and down-regulate survival pathways in a number of cancers,[23] we

Figure 1. TSP-1 inhibits MB tumor growth and metastases in vivo 1×10^5 log-phase UW426-MYC and D458 cells with stable expression of empty vector or TSP-1 were orthotopically injected into cerebella of 5–6 weeks old *Nod/Scid* mice ($n = 10$/group) and brain and spine were removed after death for histopathological studies. (A) Kaplan–Meier survival analyses of mice injected with UW426-MYC-TSP-1 and D458-TSP-1 and corresponding control lines. (B) H&E stains of whole brain and spine from mice with UW426-MYC-TSP-1, D458-TSP-1 and corresponding control lines. Insert shows higher magnification images, arrows indicate spinal metastases. (C) Tumor volume of UW426-MYC-TSP-1 and D458-TSP-1 and control xenografts. (D) Frequency of spinal metastases in mice injected with control or TSP-1-expressing UW426-MYC and D458 cell lines. Frequency of tumor metastases were determined by histological examination of the entire spinal cord. Number of mice with nonmetastatic (M0) and metastatic (M+) tumors are indicated.

also investigated whether TSP-1 had effects on MB cell survival. Specifically, we examined the effects of TSP-1 on MB cells exposed to serum starvation, radiation, and chemotherapeutic agents with different modes of actions: etoposide/VP16 (a topoisomerase inhibitor), cisplatin (an alkylating agent), and docetaxel (a mitotic inhibitor). While TSP-1 expression did not alter MB cell viability under conditions of serum starvation and after treatment with
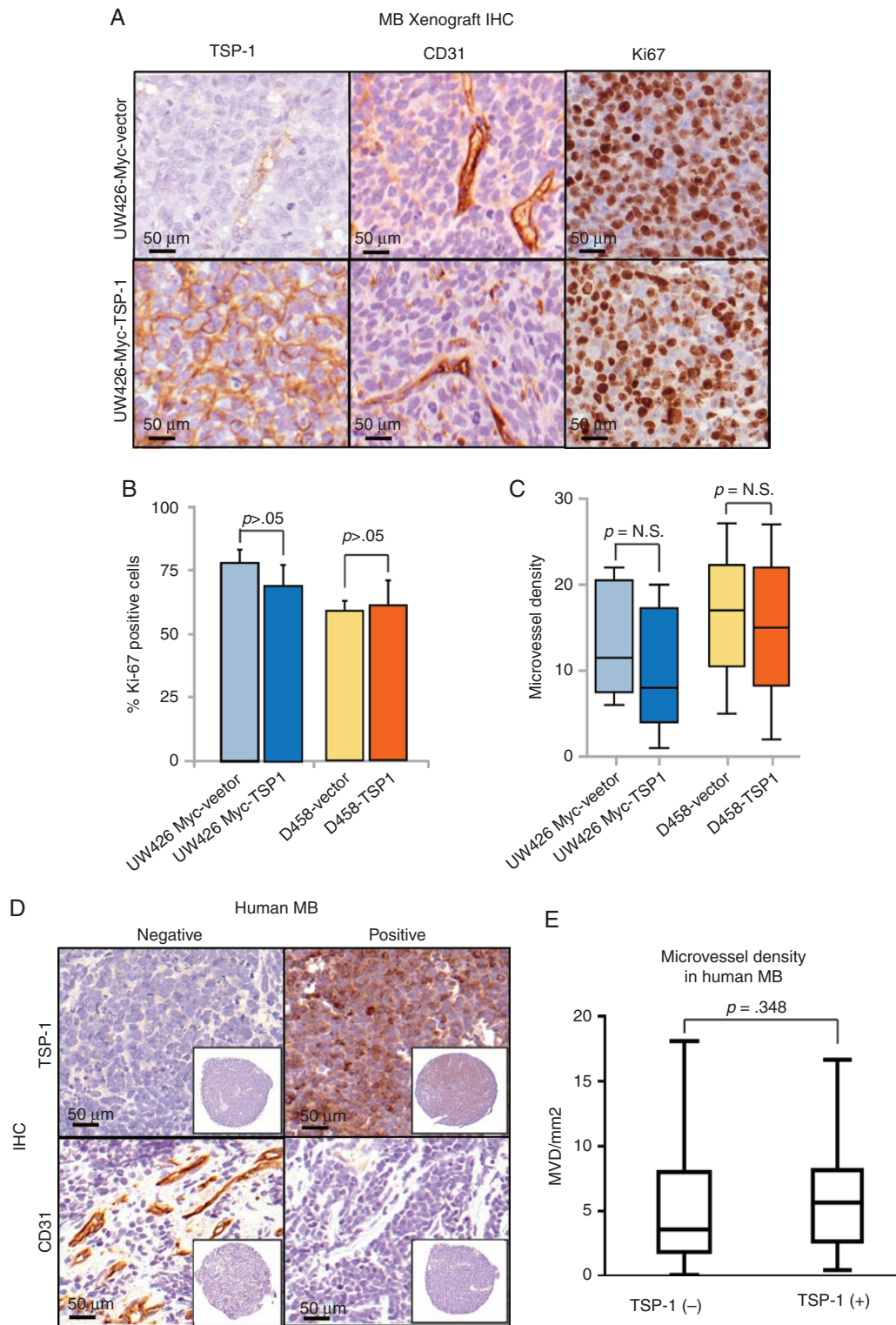
Figure 2. Immunohistochemical analyses of TSP-1, Ki-67 expression and microvessel density in MB. (A) Tumor xenografts of mice injected with UW426-MYC-vector and UW426-MYC-TSP-1 cells were stained with anti-TSP-1. Ki-67 or CD-31 antibodies. (B) Relative proliferative index (% Ki-67-positive counts) was determined by histological examination of Ki-67 stained slides while (C) MVD was determined based on number of CD31-positive vessel in 10 tumor sections/xenograft from mice injected with control and TSP-1-expressing UW426-MYC/D458 cells. (D) Representative IHC of primary human MB samples stained with anti-TSP-1 or CD31 antibodies. (E) MVD/mm^2 was determined based on counts of CD31-positive vessel in 3 random sections/primary sample (n = 225).
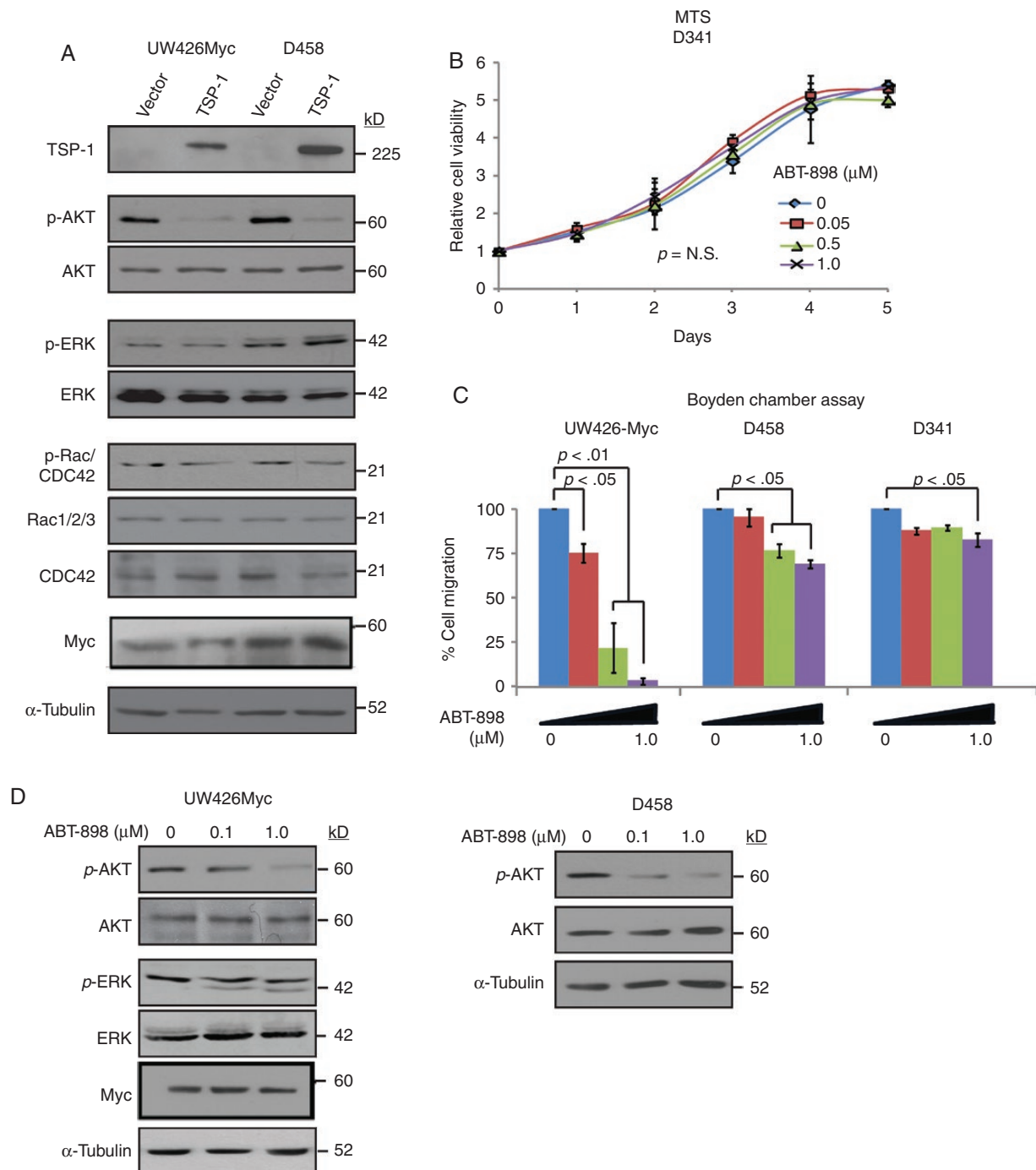
Figure 3. Down-regulation of PI3K/AKT signaling of ABT-898 inhibits MB migration. (A) Immunoblotting analyses for TSP-1, phospho- and total AKT, ERK1/2, C-MYC, Rac1/2/3, and CDC42 expression in UW426-MYC-TSP-1, D458-TSP-1 and control cell lines; tubulin was used as loading control. (B) MTS assays of D341 cells after 0, 0.05, 0.5, and 1.0 µM ABT-898 treatment. (C) 3.5×10^4 MB cells were pretreated with ABT-898 (0, 0.01, 0.5, and 1.0 µM) for 3 h and seeded in Boyden chambers; migrated cells were determined by direct cell count after 22–48 h. Percent cell migration was determined relative to controls; $n = 3$ experiments with 2 replicas/data point are summarized; error bars = SEM. (D) Immunoblotting analyses of phospho- and total AKT and ERK1/2, and C-MYC expression in UW426-MYC and D458 treated with ABT-898; tubulin served as loading control.

cisplatin and docetaxel (Supplementary Figure 3), TSP-1 expressing cells exhibited significantly reduced viability with concomitant increased PARP cleavage upon treatment with etoposide (Figure 4A). To investigate whether ABT-898 could also recapitulate the chemo-sensitizing effects

of TSP-1 expression, we established the IC25 values for etoposide in a panel of MB cell lines with high endogenous and exogenous MYC expression (Supplementary Figure 4A) and tested the cellular effects of increasing amounts of ABT-898 combined with IC25 doses of etoposide on MB.

Strikingly, the ABT-898 treatment enhanced sensitivity to etoposide in a dose-dependent manner, by up to 40% (Figure 4B, Supplementary Figure 4B). Interestingly, we also observed that TSP-1 expression, as well as ABT-898, conferred increased sensitivity to radiation in UW426-MYC and D458 cells (Figure 4C, D, Supplementary Figure 4C, D).

ABT-898 Induces Cell Death Via Inhibition of AKT Signaling in Murine Models of Group 3 Medulloblastoma

To further assess whether TSP-1 peptidomimetics would be effective therapeutics for aggressive MB, we investigated therapeutic effects of ABT-898 in two independent murine models of MYC-driven group 3 MB, named as MP and G3.[6,7] We used IHC and immunoblotting analyses to confirm that both MP and G3 cells expressed low levels of TSP-1 and high phospho-AKT levels (Figure 5A, B), similar to human MB cell lines with *MYC* amplification.[18] Both MP and G3 cells expressed high phospho-AKT levels comparable to that in D458, an *MYC* amplified MB cell line. In contrast, only low levels of phospho-AKT were observed in SHH MB cells (from *Ptch1+/-*, *Cdkn2c-/-* mice [24]) and in UW228 MB line, which has no *MYC* amplification. Treatment with ABT-898 (0.1–10 μM) for 72 h dramatically reduced the viability of both MP and G3 cells by up to 45% (Figure 5C). In contrast, ABT-898 treatment had no effects on viability of Shh mouse MB cells which have low MYC and phospho-AKT expression. To investigate the potential synergistic effects of ABT-898 with etoposide, we first determined the dose-response curve of etoposide in MP and G3 tumor cells (Supplementary Figure 4) and then tested the cellular effects of increasing amounts of ABT-898 with IC25 doses of etoposide on MP and G3 cells. Interestingly, we observed that ABT-898 enhanced cytotoxic effects of etoposide in MP and G3 cells (Figure 5D), with concomitant increased cleaved PARP and decreased phospho-AKT expression (Figure 5E). Taken together with the known role of MYC and AKT signaling in MB, these aggregate data which indicate ABT-898 mediates apoptosis in group 3 MB cells via AKT signaling further suggest MYC-driven MB may be particularly therapeutically responsive to TSP-1 peptidomimetics.

Discussion

Patients with MYC-associated group 3 MB represent a very high-risk group with frequent metastases, treatment failure, and death due to disease.[5,25,26] Thus, there has been substantial interest in developing models and therapies for this most lethal subgroup of MB. In the past decade, multiple studies have attempted to therapeutically target MYC activity,[27–30] as well as PI3K signaling[7,31–36] which has a central role in MYC-associated MB pathogenesis. TSP-1 is a potent tumor suppressor and downstream target of MYC that has been implicated in many human cancers but has not been studied in the context of MB. We previously reported that MYC-mediated silencing of TSP-1 was an important step in the pathogenesis of MYC-driven metastatic MB.[18] Here, we demonstrate that TSP-1 expression correlates with less

aggressive MB biology, and that reconstitution of TSP-1 has potent antimetastatic effects on MB progression/proliferation in vivo. Furthermore, we show pharmacologically active TSP-1 peptidomimetics can recapitulate the potent antimetastatic/cell migratory effects of TSP-1 and enhance therapeutic effects of radiation and chemotherapy in group 3 MB models. These data underscore the functional importance of TSP-1 in control of MB progression and metastases and indicate pharmacologic mimetics of TSP-1 may represent novel adjuvant therapeutics for metastatic, high-risk MB.

TSP-1 is a tumor suppressor with pleiotropic functions. Due to its potent tumor-suppressive effect, mimetics of TSP-1 have long been investigated for cancer therapies. Although TSP-1 tumor-suppressive role has been frequently associated with its anti-angiogenic properties, our data suggest that TSP-1 expression in MB does not correlate with MVD, a surrogate of angiogenesis. Our observations are consistent with reports that angiogenesis and micro-vascular density are not correlated with aggressive MB phenotypes.[37] Interestingly, TSP-1 has been suggested in advanced ovarian cancer to mediate therapeutic effects indirectly by improving drug delivery via normalization of tumor vasculature.[38]

Various pharmacologic peptidomimetics of TSP-1 including ABT-510, 526, and 898 (from Abbott Laboratories) were designed based on the sequence GVITRIR in the second type 1 TSR repeat of TSP1 which is known to bind and activate receptors such as CD36, CD47, and integrin. Studies to date reveal various cellular effects of TSP-1 and its peptidomimetics resulting in the promotion or inhibition of tumor growth. Reported antitumor effects of TSP-1 include inhibition of tumor proliferation in vivo, induction of apoptosis, chemo-sensitization, and inhibition of angiogenesis.[39–48] While we observed that TSP-1 and ABT-898 inhibit cell migration and invasion in MB, recent reports have implicated TSP-1: CD47 interaction to promote glioma invasion.[22] Although direct binding of ABT-898 to CD36 has been demonstrated,[39] whether the disparate effects of TSP-1 in glioma and MB reflects different TSP1: receptor and different tumor microenvironment interactions between gliomas and embryonal tumors are not known. It is also interesting to note that while TSP-1 expression was lowest in the group 3 MB tumors, our IHC analyses also revealed relatively low TSP-1 expression in the SHH MB subgroup in which MYCN is often overexpressed. Although MYCN has been implicated in the down-regulation of TSP-1,[15,16] our studies indicate expression of TSP-1 expression has limited effects on growth phenotypes of Daoy, a SHH MB cell line.

Human trials with ABT-510 have reported promising results in head and neck and nonsmall-cell lung cancers, lymphoma, and renal cell carcinoma.[45,46,49–52] Notably, experimental studies indicate ABT510 may have therapeutic effects glioma models[39] while phase 1 studies of glioblastoma indicate TSP-1 peptidomimetics may cross the blood-brain barrier.[47,52] We observed that ABT898 enhanced VP16 and radiation mediated cell death in human MB cells with MYC overexpression, and in cells from 2 distinct mouse models of MYC-associated group 3 MB. Notably, both ABT-898 treatment and TSP-1 expression also had distinct antimigratory/metastatic effects in vitro and in vivo. Although in vivo efficacy remains to be undertaken, these observations suggest ABT-898 and related TSP-1 mimetics
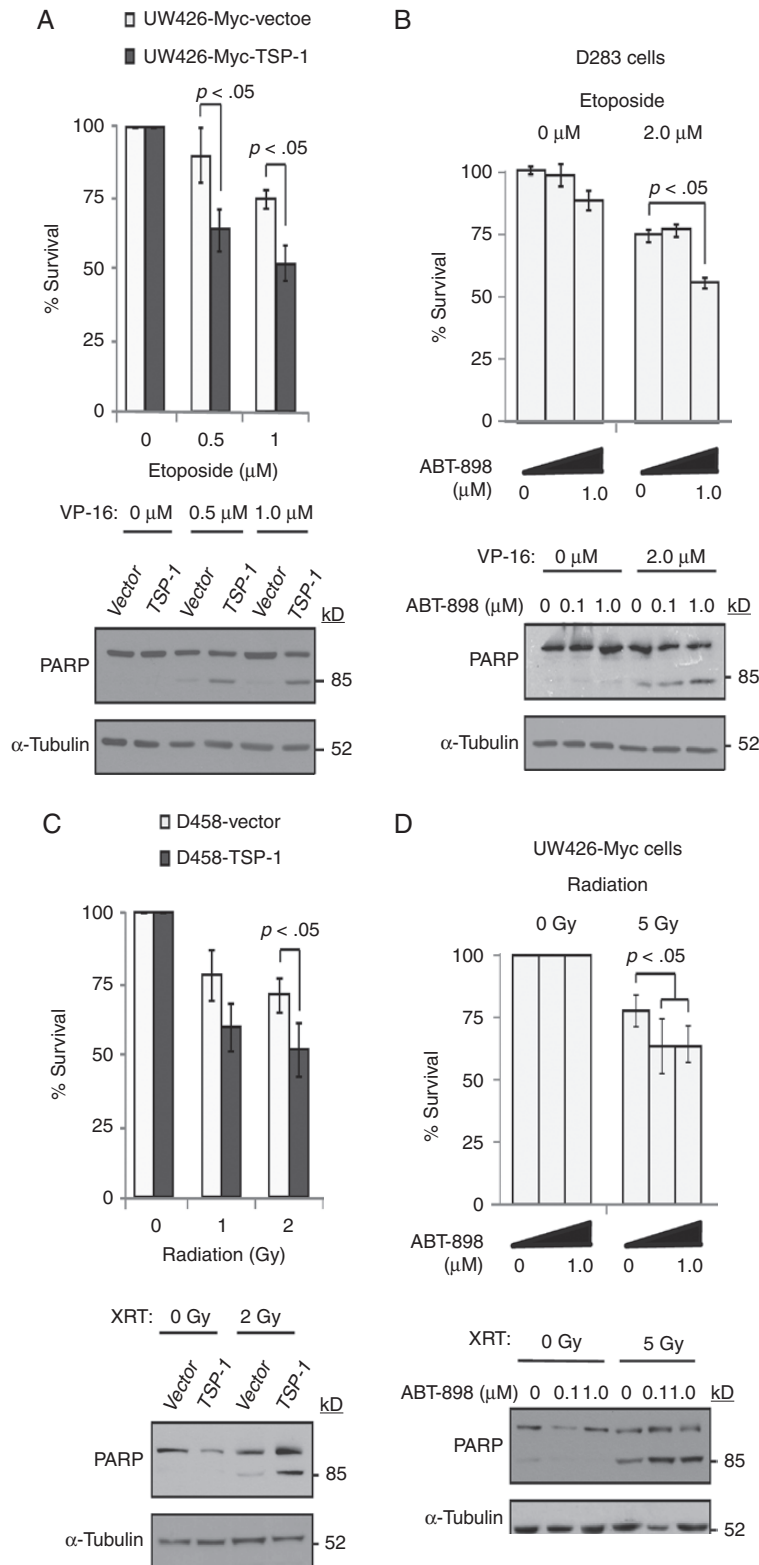
Figure 4. TSP-1 and ABT898 enhances chemo- and radio-sensitivity in MB cells. MB cells treated for 48 h with etoposide or ɣ-irradiation or combined with ABT-898 treatment were analyzed by MTS analyses and immunoblotting analyses for PARP cleavage. Relative survival of (A) UW426 MYC-vector and UW426 MYC-TSP-1 cells treated with etoposide; (B) D283 cells treated with 2.0 µM etoposide and 0, 0.1, and 1.0 µM ABT898; (C) D458-vector and D458 TSP-1 cells exposed to ɣ-irradiation; (D) UW426 MYC cells with 5 Gy ɣ-irradiation and 0, 0.1, and 1.0 µM ABT898, with corresponding PARP WB. $n = 3$ with 3 replicas/data point are summarized for each experiment; error bars = SEM.
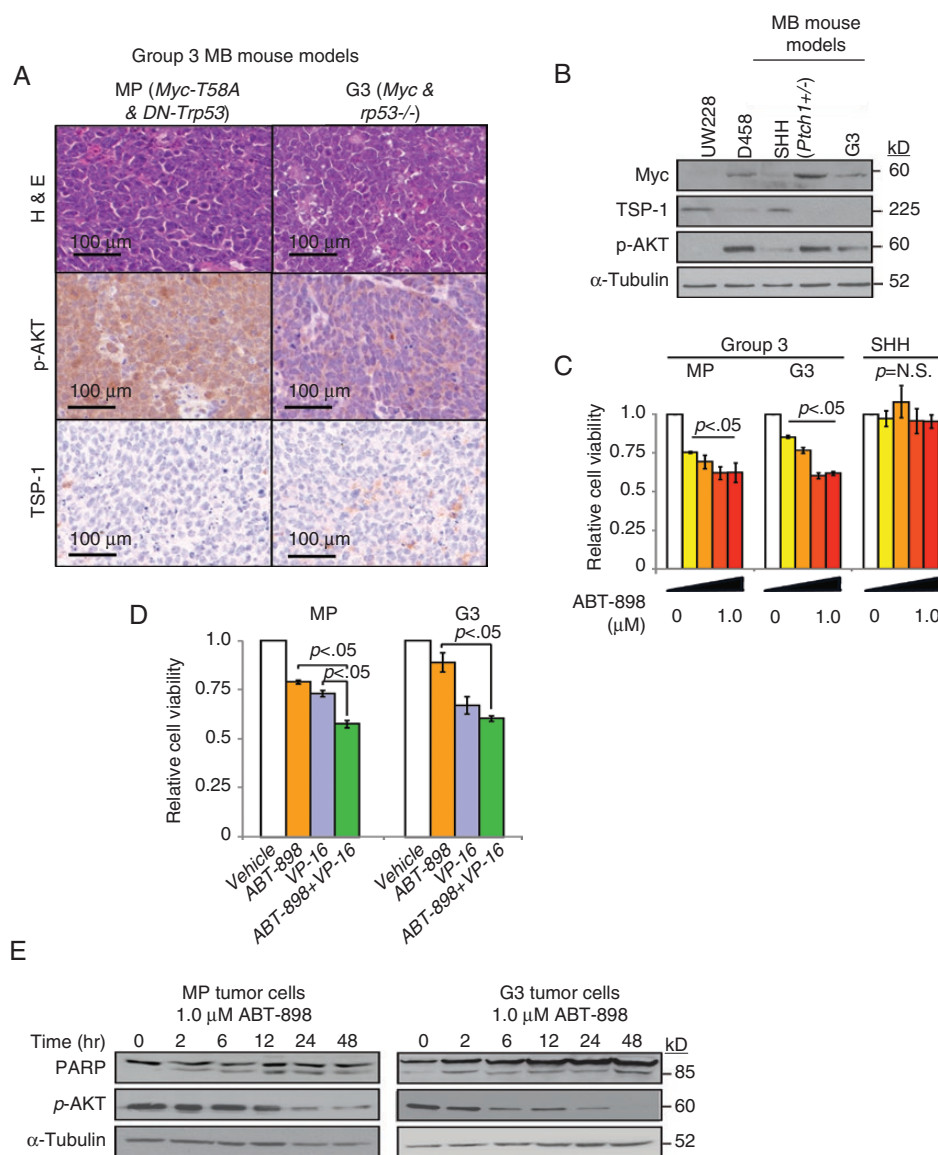
Figure 5.   ABT-898 potently inhibits AKT signaling to induce cell death in murine models of group 3 MB. (A) Representative H&E and IHC stains for phospho-AKT and TSP-1 expression in group 3 mouse MB (MP and G3) tumors. (B) Immunoblotting analyses of MYC, phospho-AKT and TSP-1 expression in UW228, D458, SHH and mouse group 3 MB tumor cells with tubulin as loading control. (C) MTS assays of murine group 3 (MP and G3) and Shh tumor cells after treatment with 0, 0.1, 0.5, 1, and 5 μM ABT898 for 72 h. Percent cell survival relative to untreated control is shown. (D) MTS assays for MP and G3 cells treated with ABT-898 (0.1 μM), or etoposide (1.0 μM) or ABT-898 (0.1 μM) combined with etoposide (1.0 μM) for 72 h. $n = 3$ with 3 replicas/data point are summarized for each experiment; error bars = SEM; N.S.: not significant. (E) Immunoblotting analyses for cleaved-PARP and phospho-AKT in MP and G3 cells after treatment with 1.0 μM ABT-898 for varying times. Tubulin was used as loading control.

may represent promising adjuvant antimetastatic agents when combined with chemo-radiation regimens for treatment of high risk, metastatic MB.

Multiple studies have implicated PI3K/AKT activation in MB and in other *MYC* and *MYCN* associated tumors.[7,53] Our data suggest that therapeutic effects of TSP-1 may be primarily mediated via PI3K signaling. ABT-898 is known to bind ß1-integrin and CD36,[54] which have both been reported to mediate their apoptotic effect by modulating AKT and FasL signaling.[55,56] Of note, although PI3K/AKT

signaling is implicated in SHH-MB, our data showed no effect of ABT-898 on SHH mouse tumor cells. These observations suggest ABT-898 or related peptidomimetics may have greater specificity for the MYC-PI3K axis in MYC driven MB than other PI3K signaling inhibitors, which frequently have off-target effects.

We observed that TSP-1 reconstitution alone did not induce cell death but augmented sensitivity specifically to chemotherapeutic agents (VP16) or radiation in MB cell lines, which suggests that TSP-1-associated cell death

may be mediated via DNA-damage response repair and/or survival pathways. As both the MP and G3 mouse MB models were derived in cell with a functionally deficient Trp53 protein, p53-independent cell death mechanisms are also likely to play a role in TSP-1 induced cell death. Despite the different AKT signaling activity levels observed in MP and G3 cells, ABT-898 triggered apoptotic cell death in vitro to a similar degree in MP and G3 cells, suggesting mechanism underlying ABT-898 pro-apoptotic effect may not be solely due to PI3K/AKT signaling. Recent studies showed that TSP-1 is associated with FasL, the ligand for the CD95 death receptor.[57] Whether or not TSP-1 exerts its apoptotic activity through the FasL apoptotic pathway in MB remains to be elucidated. It is very likely that besides inducing apoptotic cell death, ABT-898 may also have antiproliferative effects, as we observed a dramatic reduction in cell viability post-ABT898 treatment.

In summary, our collective data suggest silencing of TSP-1 contributes significantly to the metastatic, chemo- and radiation-resistant phenotypes seen in MYC-driven MB. Our observation that ABT-898 suppresses pro-survival PI3K/AKT signaling activities in two MYC-driven murine MB models suggests TSP-1 peptidomimetics as promising novel pharmacological treatment for these highly fatal tumors.

Supplementary Material

Supplementary material is available at *Neuro-Oncology Advances* online.

Keywords

AKT | medulloblastoma | MYC | PI3K | TSP-1

Conflict of interest statement. The authors disclose no potential conflicts of interest.

Authorship Statement. Concept and design: T.S.Y.C., J.H., and A.H. Provision of cell lines, study material, patient data: D.P., C.H., E.B., S.P., A.K., M.F.R., R.J.W., and J.H. Experiment execution and data interpretation: T.S.Y.C., C.H., M.L., and A.H. Manuscript writing: T.S.Y.C. and A.H. Final approval of manuscript: All authors.

References

1. Mazzola CA, Pollack IF. Medulloblastoma. *Curr Treat Options neurol.* 2003;5(3):189–198.
2. Packer RJ, Vezina G. Management of and prognosis with medulloblastoma: therapy at a crossroads. *Arch Neurol.* 2008;65(11):1419–1424.
3. Northcott PA, Korshunov A, Pfister SM, Taylor MD. The clinical implications of medulloblastoma subgroups. *Nat Rev Neurol.* 2012;8(6):340–351.
4. Ellison DW, Dalton J, Kocak M, et al. Medulloblastoma: clinicopathological correlates of SHH, WNT, and non-SHH/WNT molecular subgroups. *Acta Neuropathol.* 2011;121(3):381–396.
5. Taylor MD, Northcott PA, Korshunov A, et al. Molecular subgroups of medulloblastoma: the current consensus. *Acta Neuropathol.* 2012;123(4):465–472.
6. Kawauchi D, Robinson G, Uziel T, et al. A mouse model of the most aggressive subgroup of human medulloblastoma. *Cancer Cell.* 2012;21(2):168–180.
7. Pei Y, Moore CE, Wang J, et al. An animal model of MYC-driven medulloblastoma. *Cancer Cell.* 2012;21(2):155–167.
8. Mumert M, Dubuc A, Wu X, et al. Functional genomics identifies drivers of medulloblastoma dissemination. *Cancer Res.* 2012;72(19):4944–4953.
9. Volpert OV, Alani RM. Wiring the angiogenic switch: ras, myc, and Thrombospondin-1. *Cancer Cell.* 2003;3(3):199–200.
10. Dews M, Homayouni A, Yu D, et al. Augmentation of tumor angiogenesis by a Myc-activated microRNA cluster. *Nat Genet.* 2006;38(9):1060–1065.
11. Janz A, Sevignani C, Kenyon K, Ngo CV, Thomas-Tikhonenko A. Activation of the myc oncoprotein leads to increased turnover of thrombospondin-1 mRNA. *Nucleic Acids Res.* 2000;28(11):2268–2275.
12. Watnick RS, Rodriguez RK, Wang S, et al. Thrombospondin-1 repression is mediated via distinct mechanisms in fibroblasts and epithelial cells. *Oncogene.* 2015;34(22):2823–2835.
13. Ren B, Yee KO, Lawler J, Khosravi-Far R. Regulation of tumor angiogenesis by thrombospondin-1. *Biochim Biophys Acta.* 2006;1765(2):178–188.
14. Duquette M, Sadow PM, Lawler J, Nucera C. Thrombospondin-1 silencing down-regulates integrin expression levels in human anaplastic thyroid cancer cells with BRAF(V600E): new insights in the host tissue adaptation and homeostasis of tumor microenvironment. *Front Endocrinol (Lausanne).* 2013;4:189.
15. Kazerounian S, Yee KO, Lawler J. Thrombospondins in cancer. *Cell Mol Life Sci.* 2008;65(5):700–712.
16. Mirochnik Y, Kwiatek A, Volpert OV. Thrombospondin and apoptosis: molecular mechanisms and use for design of complementation treatments. *Curr Drug Targets.* 2008;9(10):851–862.
17. Rusk A, McKeegan E, Haviv F, et al. Cooperative activity of cytotoxic chemotherapy with antiangiogenic thrombospondin-l peptides, ABT-526 in pet dogs with relapsed lymphoma. *Clin Cancer Res.* 2006;12(24):7456–64.
18. Zhou L, Picard D, Ra YS, et al. Silencing of thrombospondin-1 is critical for myc-induced metastatic phenotypes in medulloblastoma. *Cancer Res.* 2010;70(20):8199–8210.
19. Huang A, Ho CS, Ponzielli R, et al. Identification of a novel c-Myc protein interactor, JPO2, with transforming activity in medulloblastoma cells. *Cancer Res.* 2005;65(13):5607–5619.
20. Włodarski P, Grajkowska W, Łojek M, Rainko K, Jóźwiak J. Activation of Akt and Erk pathways in medulloblastoma. *Folia Neuropathol.* 2006;44(3):214–220.

21. Parri M, Chiarugi P. Rac and Rho GTPases in cancer cell motility control. *Cell Commun Signal*. 2010;8:23.

22. Daubon T, Leon C, Clarke K, et al. Deciphering the complex role of therombospondin-1 in glioblastoma development. *Nature Comm*. 2019;10:1146.

23. Lawler J. Thrombospondin-1 as an endogenous inhibitor of angiogenesis and tumor growth. *J Cell Mol Med*. 2002;6(1):1–12.

24. Uziel T, Zindy F, Xie S, et al. The tumor suppressors Ink4c and p53 collaborate independently with Patched to suppress medulloblastoma formation. *Genes Dev*. 2005;19(22):2656–2667.

25. Tomlinson FH, Jenkins RB, Scheithauer BW, et al. Aggressive medulloblastoma with high-level N-myc amplification. *Mayo Clin Proc*. 1994;69(4):359–365.

26. von Hoff K, Hartmann W, von Bueren AO, et al. Large cell/anaplastic medulloblastoma: outcome according to myc status, histopathological, and clinical risk factors. *Pediatr Blood Cancer*. 2010;54(3):369–376.

27. Bandopadhayay P, Bergthold G, Nguyen B, et al. BET bromodomain inhibition of MYC-amplified medulloblastoma. *Clin Cancer Res*. 2014;20(4):912–925.

28. Diaz RJ, Golbourn B, Faria C, et al. Mechanism of action and therapeutic efficacy of Aurora kinase B inhibition in MYC overexpressing medulloblastoma. *Oncotarget*. 2015;6(5):3359–3374.

29. Morfouace M, Shelat A, Jacus M, et al. Pemetrexed and gemcitabine as combination therapy for the treatment of Group3 medulloblastoma. *Cancer Cell*. 2014;25(4):516–529.

30. Faria CC, Agnihotri S, Mack SC, et al. Identification of alsterpaullone as a novel small molecule inhibitor to target group 3 medulloblastoma. *Oncotarget*. 2015;6(25):21718–21729.

31. Ehrhardt M, Craveiro RB, Holst MI, Pietsch T, Dilloo D. The PI3K inhibitor GDC-0941 displays promising in vitro and in vivo efficacy for targeted medulloblastoma therapy. *Oncotarget*. 2015;6(2):802–813.

32. Baryawno N, Sveinbjörnsson B, Eksborg S, Chen CS, Kogner P, Johnsen JI. Small-molecule inhibitors of phosphatidylinositol 3-kinase/Akt signaling inhibit Wnt/beta-catenin pathway cross-talk and suppress medulloblastoma growth. *Cancer Res*. 2010;70(1):266–276.

33. Wojtalla A, Salm F, Christiansen DG, et al. Novel agents targeting the IGF-1R/PI3K pathway impair cell proliferation and survival in subsets of medulloblastoma and neuroblastoma. *PLos One*. 2012;7(10):e47109.

34. Salm F, Dimitrova V, von Bueren AO, et al. The phosphoinositide 3-Kinase p110α isoform regulates leukemia inhibitory factor receptor expression via c-Myc and miR-125b to promote cell proliferation in medulloblastoma. *PLos One*. 2015;10(4):e0123958.

35. Guerreiro AS, Fattet S, Kulesza DW, et al. A sensitized RNA interference screen identifies a novel role for the PI3K p110γ isoform in medulloblastoma cell proliferation and chemoresistance. *Mol Cancer Res*. 2011;9(7):925–935.

36. Guerreiro AS, Fattet S, Fischer B, et al. Targeting the PI3K p110alpha isoform inhibits medulloblastoma proliferation, chemoresistance, and migration. *Clin Cancer Res*. 2008;14(21):6761–6769.

37. Grizzi F, Weber C, Di Ieva A. Antiangiogenic strategies in medulloblastoma: reality or mystery. *Pediatr Res*. 2008;63(5):584–590.

38. Campbell N, Greenaway J, Henkin J, Petrik J. ABT-898 induces tumor regression and prolongs survival in a mouse model of epithelial ovarian cancer. *Mol Cancer Ther*. 2011;10(10):1876–1885.

39. Anderson JC, Grammer JR, Wang W, et al. ABT-510, a modified type 1 repeat peptide of thrombospondin, inhibits malignant glioma growth in vivo by inhibiting angiogenesis. *Cancer Biol Ther*. 2007;6(3):454–462.

40. Campbell NE, Greenaway J, Henkin J, Moorehead RA, Petrik J. The thrombospondin-1 mimetic ABT-510 increases the uptake and effectiveness of cisplatin and paclitaxel in a mouse model of epithelial ovarian cancer. *Neoplasia*. 2010;12(3):275–283.

41. Greenaway J, Henkin J, Lawler J, Moorehead R, Petrik J. ABT-510 induces tumor cell apoptosis and inhibits ovarian tumor growth in an orthotopic, syngeneic model of epithelial ovarian cancer. *Mol Cancer Ther*. 2009;8(1):64–74.

42. Baek KH, Bhang D, Zaslavsky A, et al. Thrombospondin-1 mediates oncogenic Ras-induced senescence in premalignant lung tumors. *J Clin Invest*. 2013;123(10):4375–4389.

43. Isenberg JS, Yu C, Roberts DD. Differential effects of ABT-510 and a CD36-binding peptide derived from the type 1 repeats of thrombospondin-1 on fatty acid uptake, nitric oxide signaling, and caspase activation in vascular cells. *Biochem Pharmacol*. 2008;75(4):875–882.

44. Recouvreux MV, Camilletti MA, Rifkin DB, Becu-Villalobos D, Díaz-Torga G. Thrombospondin-1 (TSP-1) analogs ABT-510 and ABT-898 inhibit prolactinoma growth and recover active pituitary transforming growth factor-β1 (TGF-β1). *Endocrinology*. 2012;153(8):3861–3871.

45. Haviv F, Bradley MF, Kalvin DM, et al. Thrombospondin-1 mimetic peptide inhibitors of angiogenesis and tumor growth: design, synthesis, and optimization of pharmacokinetics and biological activities. *J Med Chem*. 2005;48(8):2838–2846.

46. Yang Q, Tian Y, Liu S, et al. Thrombospondin-1 peptide ABT-510 combined with valproic acid is an effective antiangiogenesis strategy in neuroblastoma. *Cancer Res*. 2007;67(4):1716–1724.

47. Sahora AI, Rusk AW, Henkin J, McKeegan EM, Shi Y, Khanna C. Prospective study of thrombospondin-1 mimetic peptides, ABT-510 and ABT-898, in dogs with soft tissue sarcoma. *J Vet Intern Med*. 2012;26(5):1169–1176.

48. Rusk A, McKeegan E, Haviv F, Majest S, Henkin J, Khanna C. Preclinical evaluation of antiangiogenic thrombospondin-1 peptide mimetics, ABT-526 and ABT-510, in companion dogs with naturally occurring cancers. *Clin Cancer Res*. 2006;12(24):7444–7455.

49. Gordon MS, Mendelson D, Carr R, et al. A phase 1 trial of 2 dose schedules of ABT-510, an antiangiogenic, thrombospondin-1-mimetic peptide, in patients with advanced cancer. *Cancer*. 2008;113(12):3420–3429.

50. Ebbinghaus S, Hussain M, Tannir N, et al. Phase 2 study of ABT-510 in patients with previously untreated advanced renal cell carcinoma. *Clin Cancer Res*. 2007;13(22 Pt 1):6689–6695.

51. Markovic SN, Suman VJ, Rao RA, et al. A phase II study of ABT-510 (thrombospondin-1 analog) for the treatment of metastatic melanoma. *Am J Clin Oncol*. 2007;30(3):303–309.

52. Nabors LB, Fiveash JB, Markert JM, et al. A phase 1 trial of ABT-510 concurrent with standard chemoradiation for patients with newly diagnosed glioblastoma. *Arch Neurol*. 2010;67(3):313–319.

53. Buonamici S, Williams J, Morrissey M, et al. Interfering with resistance to smoothened antagonists by inhibition of the PI3K pathway in medulloblastoma. *Sci Transl Med*. 2010;2(51):51ra70.

54. Febbraio M, Hajjar DP, Silverstein RL. CD36: a class B scavenger receptor involved in angiogenesis, atherosclerosis, inflammation, and lipid metabolism. *J Clin Invest*. 2001;108(6):785–791.

55. Jiménez B, Volpert OV, Crawford SE, Febbraio M, Silverstein RL, Bouck N. Signals leading to apoptosis-dependent inhibition of neovascularization by thrombospondin-1. *Nat Med*. 2000;6(1):41–48.

56. Volpert OV, Zaichuk T, Zhou W, et al. Inducer-stimulated Fas targets activated endothelium for destruction by anti-angiogenic thrombospondin-1 and pigment epithelium-derived factor. *Nat Med*. 2002;8(4):349–357.

57. Quesada AJ, Nelius T, Yap R, et al. In vivo upregulation of CD95 and CD95L causes synergistic inhibition of angiogenesis by TSP1 peptide and metronomic doxorubicin treatment. *Cell Death Differ*. 2005;12(6):649–658.